

DEVELOPMENT OF TRANSFORMATIVE CAVITY PROCESSING – SUPERIORITY OF ELECTROPOLISHING ON HIGH GRADIENT PERFORMANCE OVER BUFFERED CHEMICAL POLISHING AT LOW FREQUENCY (322 MHz)*

K. Saito[†], C. Compton, W. Chang, K. Elliott, T. Konomi, S-H. Kim, W. Hartung, E. Metzgar, S. Miller, L. Popielarski, A. Taylor, T. Xu
MSU, FRIB, East Lansing, MI, USA

Abstract

A DOE grant R&D titled “Development of Transformative Preparation Technology to Push up High Q/G Performance of FRIB Spare HWR Cryomodule Cavities” is ongoing at FRIB. This R&D is for 2 years since September 2022, until August 2024. This project focusses to develop the preparation for the high Q&G 0.53 half wave resonators to build high gradient spare cryomodule. This project proposes four objectives: 1) demonstration of superiority on high gradient performance of electropolishing (EP) over buffered chemical polishing on medium beta half-wave cavities at 322 MHz, 2) high Q_0 performance by the local magnetic shield, 3) Development of HFQS-free BCP, and 4) Wet N-doping method. This paper will report the result of first object, and some magnetic shield design for the object 2.

INTRODUCTION

FRIB has switched to user operation from the commissioning phase. In this stage, the reliability of the machine operation is the first priority. This proposal focuses on the FRIB machine maintenance strategy. Some FRIB cavities may have degrade the performance during a long machine operation, and the cryomodule(s) including the degraded cavity(s) would be replaced by spare cryomodule (s). So far, of the six FRIB cryomodule families, three have certified spares that were fabricated as part of the project.

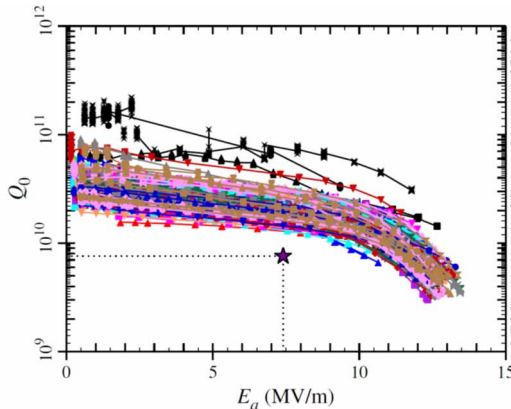


Figure 1: VTA cavity performance with FRIB beta 0.53 half wave resonator (HWRs).

* Work supported by the U.S. Department of Energy Office Science DE-SC114424

[†] email address: saito@frib.msu.edu

line. The spare beta 0.29 and 0.53 cryomodules were not included in the baseline, and are being planned as future scope of FRIB machine maintenance strategy. These spare cryomodules will utilize existing cavities that had been fabricated as part of production contracts. These spare cryomodules or cavities must have an enough performance margin against the degradation, for machine operation.

The goal of this proposal is to produce 0.53 HWRs operateable at acceleration gradients > 10 MV/m, keeping a high $Q_0 > 1 E + 10$ for the restoring or construction of FRIB spare cryomodules. The FRIB production cavities were all treated with BCP, as the result the usable gradient was limited by field emission or high field Q-slope (HFQS) in many cases. At first we will develop transformative processing technique for medium beta cavities, in order to mitigate or eliminate these issues.

PROBLEM STATEMENT/ CURRENT OF THE FIELD

Field limitation of FRIB Cavities

VTA cavity performance of all FRIB beta 0.53 HWRs are shown in Fig. 1 as an example. Note that FRIB cavities were treated by bulk BCP (120 μ m), hydrogen degassing (600 $^{\circ}$ C 10 hr), light BCP (20 μ m), high pressure rinsing (HWR) and cavity clean assembled in a class 100 cleanroom. A detailed FRIB VTA cavity data analysis summarized in Table 1 with the FRIB cavity performance limitation [1]. The dominant limitations are field emission (35% in average over four cavity families), and HFQS (54% in average over four cavity families).

Table 1: Statistics of Field Limitation of FRIB Cavities

Type	QWR-0.041	QWR-0.085	HWR-0.29	HWR-0.53
Total number of certificated cavities	16	106	72	148
1. Quench $< B_p=85$ mT	1 (0.6%)	0 (0%)	13 (18%)	2 (0.1%)
2. Field emission X-ray below $B_p=85$ mT	3 (19%)	41(39%)	21 (29%)	109 (74%)
3. Pure HFQS, including quench $> B_p=85$ mT	9 (56%)	26 (25%)	32 (44%)	21 (14%)
4. Suspicious HFQS X-ray onset $> B_p=85$ mT	3 (19%)	39 (37%)	6 (8%)	16 (11%)
HFQS total (3+4)	12 (75%)	65 (61%)	38 (53%)	37 (25%)

Proposed Solution

Objective 1: EP or EP+LTB Electropolishing provide a smooth surface finishing, which can make it easier to remove particle contamination by HPR. This could mitigated the field emission. As well established in the ILC cavity development, the post EP low temperature bake (LTB) can eliminate the HFQS [2]. So the first solution

Content from this work may be used under the terms of the CC BY 4.0 licence (© 2023). Any distribution of this work must maintain attribution to the author(s), title of the work, publisher, and DOI

should be EP or combination of EP and post EP LTB. EP on the HWR at 162.5 MHz was has been performed at ANL and high gradient performance was confirmed, however post EP LTB was not carried out in the study [3]. Objective one will pursue the impact of the post EP LTB.

Objective 2: Local magnetic Shield Considering cryoload, at the high gradient operation, intrinsic Q_0 must be improved proportional to the operation gradient square. Even succeed in the flat Q_0 performance by EP or EP + LTB, still medium Q slope will limit the high gradient operation. Overall Q_0 performance needs to be pushed up. To do so, the residual surface resistance should be small. One consideration to achieve is to reduce the residual surface resistance by decreasing the flux trapping due to the ambient magnetic field. Local magnetic shield would be effective to achieve this result. The second objective to provide high Q_0 performance is install a local magnetic shield surrounding the cavity.

Objective 3: HFQS free BCP EP may not remove uniformly complicate geometry such as medium beta HWRs. Chemical polishing is an attractive preparation technique on this point. However, current BCP produces the HFQS which cannot be eliminated by post BCP LTB. A PhD program at MSU focused to investigate the cause of this HFQS and concluded that nitrogen contamination due to the nitric acid in the BCP mixture is the root cause [4]. In addition, a new BCP mixture without nitric acid has been developed in this program [5]. If not contained the nitric acid, the behavior of the HFQS will be same as EP case: Oxygen contamination, therefore post BCP LTB could eliminate the HFQS. We will apply this new acid to the medium beta cavities. This study is planned to start after this conference.

Objective 4: Wet N Doping We mined old data and found out a potential N-doping by EP. If this succeeds, any annealing process in the vacuum furnace at 800 – 900 °C would not be necessary. N-doping could be done just by EP. This study is also planned to start after this conference.

PROCEDURES

An EP facility was built in 2022 at FRIB SRF Highbay for the future SRF development, collaborating ANL [6]. We have completed the commissioning by end of Dec. 2022. In Mar. 2023 we applied bulk EP (120 μm) on SC53-159 FRIB 0.53 HWR. Table 2 shows the EP parameters reached during this EP. An optimum current density of 30 mA/cm² was secured. The material removal matched well the weight measurement result, and the calculation from total charge.

Table 2: EP Parameters on SC53-159

EP voltage [V]	Average Current [A]	Average current density [mA/cm ²]	Acid temperature [°C]	Flow rate [L/min]	Rotational speed [turn/min]	Total EP time [hr]	Material removal	
							From total charge	From weight deference
16	269	29	Inlet 17 °C Outlet 27°C	2.6	1	8.5	119.9 μm	122.9 μm

Borescope Inspection

Before EP Borescope inspection was performed before the bulk EP. Several potential surface damages were detected like pits, and sputter balls nearby electron beam welding seams. The defects were all mechanically ground off. Figures 2 and 3 show typical defects and the surface after grinding.

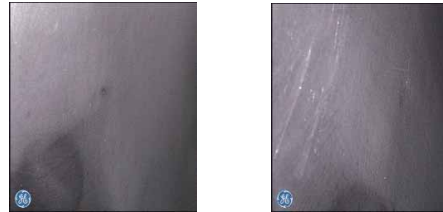


Figure 2: Typical potential surface damage: pit (left), the surface after mechanically ground off (right).

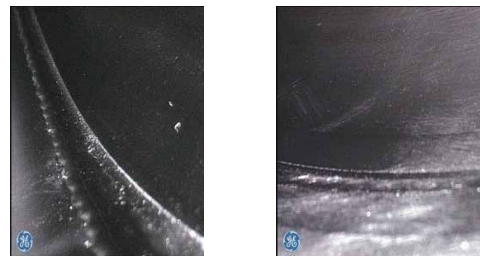


Figure 3: Typical potential surface damage: sputter ball (left), the surface after mechanically ground off (right).

After EP

Figure 4 shows a typical surface after 120 μm EP. The surface was very shiny, mirror like, and smooth.

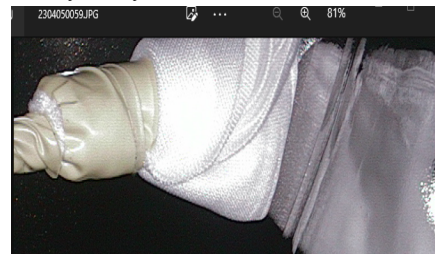


Figure 4: After EP 120μm, the EBW seam area in Fig. 3.

Hydrogen Degassing

The bulk EP'd SC53-159 was ultrasonic rinsed for 1 hr using the detergent Micro90 1%, and dried in the cleanroom. The cavity was hydrogen degassed at 600 °C for 10 hr, as following the router of the FRIB production cavities. The cavity was exposed to 350 °C for 11.5 hr before 600 °C. Figure 5 shows the RGA output during the degassing. Hydrogen was degassed, from 2 E-5 Torr to 4 E-6 by end of the degassing.

Final Light EP and Clean Assembly

The cavity lightly EP'd for 20μm removal by the same EP condition at the bulk EP, then rinsed using ultrapure water, ultrasonic rinsing with Micro90-1%, and high pressure water rinsed for 2 hr. The cavity was dried in the class 10 cleanroom for one night, then assembled in the cleanroom.

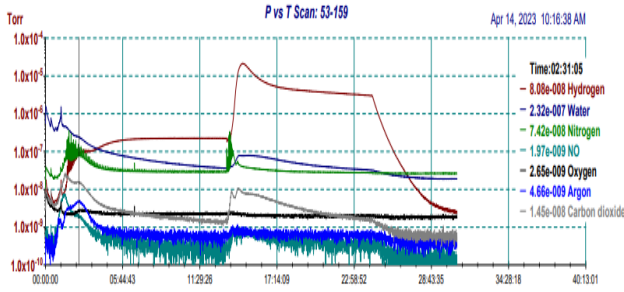


Figure 5: AGA data during the hydrogen degassing. The cavity was exposed at 350 °C for 11.5 hr, the 600 °C for 10 hr.

VTA TEST RESULT

VTA Test Procedure

SC53-159 was first VTA tested at 4.3 K, and ~ 2 K to measure the cavity performance by EP (159 EP). The cooling cooldown scheme in this VTA is same as the FRIB production cavity: fast cooldown but no considered about flux trapping expel.

After the first VTA test, the cavity was warmed up to RT in order to perform post EP LTB. The LTB was carried out at 120 °C for 48 hr. Nitrogen gas was introduced into the LHe jacket of the cavity. The nitrogen gas was heated up 120 °C by a heater dressed on the jacket.

After the LTB, the cavity was again VTA tested (159 baked).

Temperature Dependence of Surface Resistance

Comparison of the temperature dependence of surface resistance between EP and post EP LTB is shown in Fig. 6. The surface resistance was BCS fitted using the formula:

$$R_s = \frac{A}{T} \cdot \exp\left(-\frac{\Delta}{k_B T}\right) + R_{res}. \quad (1)$$

The fitting results are summarized in Table 3. Post EP LTB reduces the BCS surface resistance by a factor 1.4, of which result is similar to the result on 1.3 GHz ILC cavities [2].

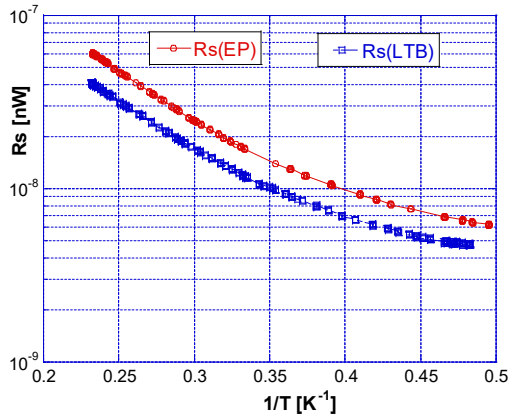


Figure 6: Comparison of the temperature dependence of surface resistance between EP and Post EP LTB.

This is interpreted to be caused by the shorter mean free path length by Oxygen diffusion from the RF penetration depth to deeper layer [7].

Fundamental SRF research and development

High quality factors/high gradients

Table 3: BCS Fit Results in Fig.6.

	EP	Post EP LTB
A [nΩ]	2.114e-5	8.709e-6
Δ/k _B	19.42	17.32
R _{res} [nΩ]	5.90	3.164

Comparison of Q₀ vs E_a Curve at 4.3 K between EP and Post EP LTB

Figure 7 compares the Q₀ vs E_a curve for the EP and post EP LTB. Even low frequency 322 MHz, the BCS surface resistance is dominant at 4.3 K. The Q₀ value of the post LTB is higher than EP by the benefit of LTB, and the medium Q slope also mitigated. The field was limited by the available RF power, and not due to quench.

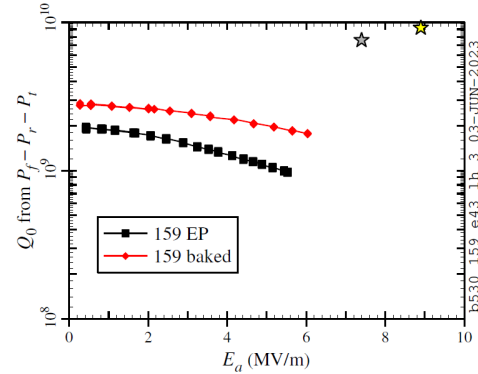


Figure 7: Comparison of the Q₀ vs E_a curve between EP (159 EP) and post EP LTB (159 baked) at 4.3 K.

Comparison of Q₀ vs E_a Curve at ~ 2 K between EP and Post EP LTB

Figure 8 compares the Q₀ vs E_a curve measured at ~ 2 K. We can see that HFQS is eliminated by post EP LTB, however this data includes an uncertainty due to the bath temperature: helium bath temperature was 2 – 2.4 K for EP case and 1.98 – 2.2 K for post LTB. To exclude the temperature depend BCS surface resistance, Q_{res} was calculated as following:

$$\frac{1}{Q_0(T)} = \frac{1}{Q_{BCS}(T)} + \frac{1}{Q_{res}(T)}, \quad (2)$$

$$Q_{BCS}(T) = \frac{G}{R_{BCS}(T)}, \quad (3)$$

$$R_{BCS}(T) = \frac{A}{T} \cdot \exp\left(-\frac{\Delta}{k_B T}\right). \quad (4)$$

G is a geometrical factor, 107.4 Ω for SC53-159. Eq. (4) is obtained from the data fitting result shown in Fig. 6, and Table 3. The Q_{res} calculation is shown in Fig. 9. Q_{res} is very similar to the Fig. 8. From this result, we believe that HFQS appeared on EP'd cavity has been eliminated by the post EP LTB. This fact is well known in the 1.3 GHz ILC cavities [2]. The high Q&G cavity performance was reached up to 15.5 MV/m, Bp = 133 mT by the EP + post EP LTB. Bp/E_a is 8.6 mT/ (MV/m) for this cavity. This maximum gradient limitation is the available RF power and not due to cavity quench.

Content from this work may be used under the terms of the CC BY 4.0 licence (© 2023). Any distribution of this work must maintain attribution to the author(s), title of the work, publisher, and DOI

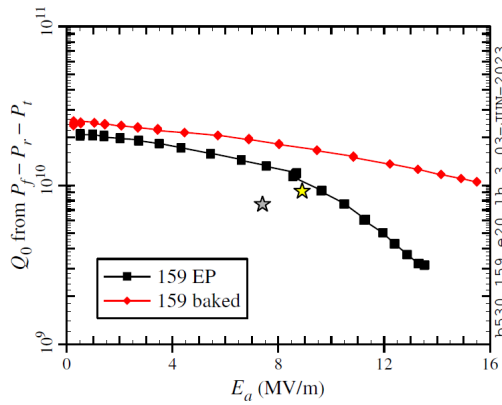


Figure 8: Comparison of the Q_0 vs E_a curve between EP and post EP LTB at ~ 2 K.

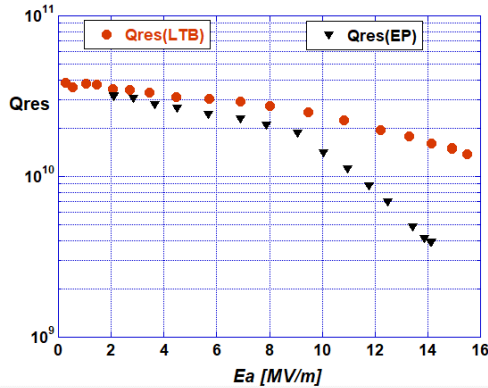


Figure 9: Comparison of Q_{res} between EP and LTB.

COMPARISON OF POST EP LTB AND BCP

Surface Resistance

Figure 10 compares temperature dependence of the surface resistance at low gradient between post EP LTB and BCP (FRIB production cavities). Thanks to LTB, the surface resistance is small but high at lower temperature, due to the higher residual resistance in post EP LTB.

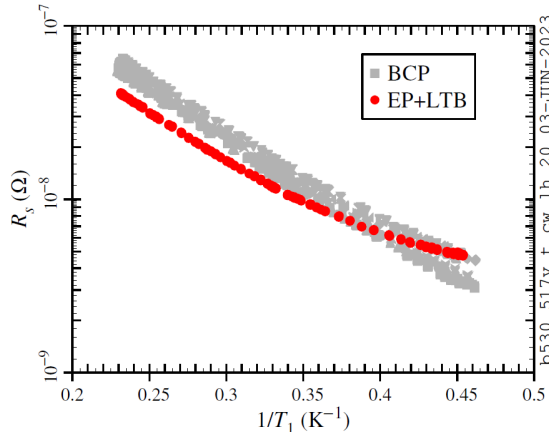


Figure 10: Comparison of temperature dependence of surface resistance between EP+LTB and BCP.

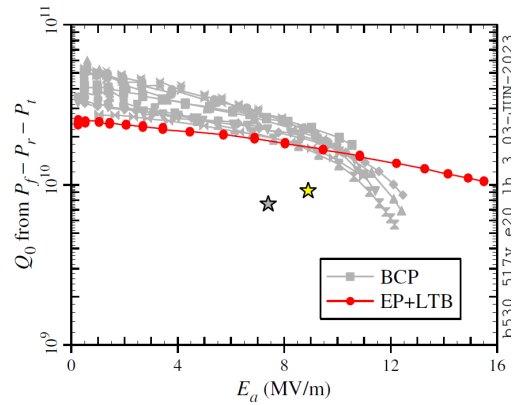


Figure 11: Comparison between EP+LTB and BCP result in FRIB production cavities.

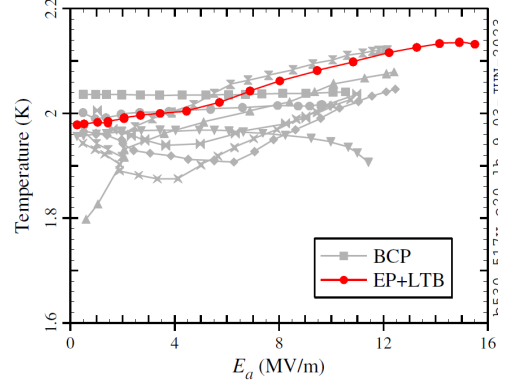


Figure 12: Helium bath temperature during Q_0 vs E_a curve measurement with FRIB BCP'd production cavities and this test (EP+LTB).

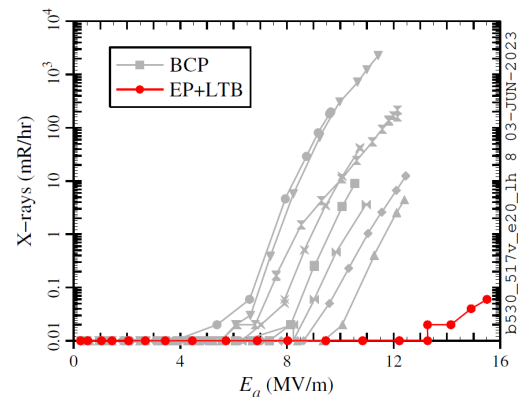


Figure 13: Comparison of X-ray between EP'd and post EP LTB'd.

Comparison of Q_0 vs E_a Curve

Figure 11 compares BCP'd FRIB production cavities, and Post EP LTB'd cavity. As seen in Fig. 12, the bath temperature during Q_0 vs E_a measurement is high in this test compared to FRIB production cavities. So there is an uncertainty to conclude Q_0 performance in Fig. 11, but there is no doubt in high gradient performance with post EP LTB.

Comparison of X-ray

Figure 13 compares X-ray between post EP LTB'd cavity and BCP'd production cavities. EP and post EP+LTB

produced very tiny X-rays < 0.1 mR/hr as shown in Fig. 13 (post EP+LTB case). These tiny X-rays don't appear as Q_0 load in Q_0 vs E_a curve. Usually X-ray load appears at X-ray > 10 mR/hr in our VTA measurement. In BCP case, the amount of X-ray is stronger by two or three order of magnitude than EP+LTB case, and the onset of X-ray is distributed at lower gradient area. As expected, FE issue is very much mitigated thanks to the soother surface by EP.

DISCUSSION

EP (+LTB) Superiority on High Q & G Cavity Performance over BCP

In Fig. 11, one can conclude that the superiority of EP (+LTB) over BCP on high gradient performance has been reconfirmed at medium beta cavity at 322 MHz. High field performance by electropolishing HWR has been demonstrated in ANL [3]. However, that study did not investigate post EP LTB. Incredibly this is the first result on medium beta cavity on post EP LTB, because EP is not yet so popular in the low/medium beta cavity community. The superiority of EP on high gradient performance over BCP was published in 1997 based on the 1.3 GHz ILC cavity studies [8]. Our results show that this holds true over a wide frequency range regardless of the cavity shape.

In the low/medium beta cavity community, the guideline in cavity design is to set the operation gradient so that the surface magnetic field does not exceed 70 mT. Really the HFQS is observed from 68.8 mT (8 MV/m) on FRIB 0.53 production HWRs, as seen in Fig.11. FRIB cavity designs followed to this guideline in the recommendations of ASAC. The result of this time is that as long as electropolishing is used, that guideline will be abolished, and it will be possible to design cavities with higher operation gradient. This will have a great impact on the future design of heavy ion accelerator.

PROGRESS OF OBJECTIVE 2

The above result is good for 10 MV/m operation, but Q_0 might be not sufficient for gradient operation, for instance 14 MV/m, if considered of much higher gradient operation. Q_0 acceptable to the current FRIB cryoplant capability for 14 MV/m operation is to be 3.3×10^{10} . R_{res} and R_{BCS} both have to be reduced very much. Decreasing BCS surface resistance is a topic in the objective 4. To reduce the residual surface resistance, we have to understand the origin but one potential is the ambient magnetic field. Objective 2 is developing a local magnetic shield reduce to ambient field < 0.1 mG in order to sufficiently exclude this origin.

Local Magnetic Shield Design

We have designed a local magnetic shield shown in Fig. 14. Figure 15 shows the current ambient magnetic field measured in our VTA Dewar. The ambient field is 2-5 mT at the cavity effective zone. Considering this field distribution and the field dependence of the permeability of shield material [9], we estimated the ambient magnetic field in the local magnetic field designed using CST. The simulation result is shown in Fig. 16. The ambient field

may be reduced to < 0.1 mT in the effective cavity zone. The frequency of SC53-159 is 322 MHz, and the issue of the flux trapping is not so large. Such a low ambient field (< 0.1 mG) has no contribution on R_{res} , thus the ambient issue will be perfectly excluded from the origin of R_{res} , except the issue of the thermo-current of the bimetal like Nb-NbTi (cavity flange area).

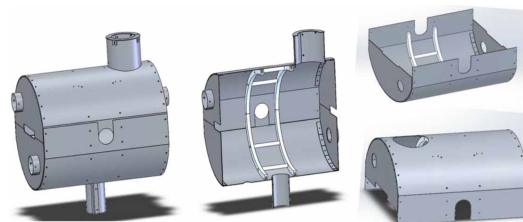


Figure 14: Local magnetic shield design in the object 2.

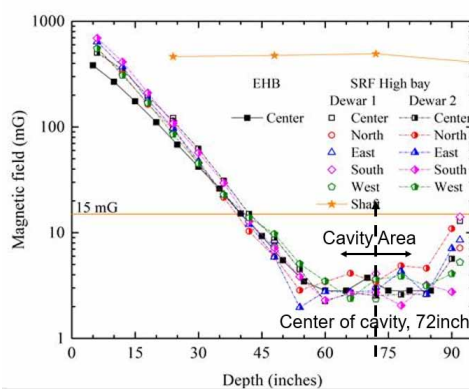


Figure 15: Measured ambient magnetic field in a Dewar in SRF Highbay.

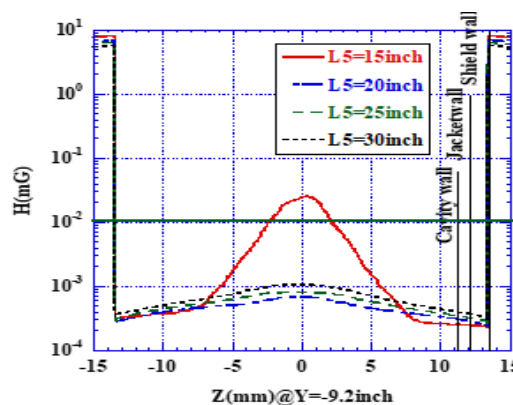


Figure 16: Simulation of the ambient field in the local magnetic shield designed in Fig. 14, with dependence of the length of the chimney of the LHe port.

SUMMARY

The superiority of EP (+LTB) on high gradient cavity performance over BCP has been confirmed on HWR with frequency 322 MHz, as similar to 1.3 ILC cavities. As a result, HFQS is eliminated by post EP LTB, the cavity performance resulted in flat Q_0 up to the maximum gradient > 15.5 MV/m. A transformative preparation technology has been successfully developed for the FRIB maintenance strategy.

REFERENCES

- [1] Cong Zhang *et al.*, “Certification testing of production superconducting quarter-wave and half-wave resonators for FRIB”, *Nucl. Instrum. Methods Phys. Res., Sect. A*, vol. 1014, p. 165675, 2021. doi:10.1016/j.nima.2021.165675
- [2] K. Saito and P. Kneisel, “Temperature dependence of the surface resistance of niobium at 1300 MHz - comparison to BCS theory”, in *Proc. SRF’99*, Santa Fe, NM, USA, Nov. 1999, paper TUP031, pp. 277-282.
<https://jacow.org/SRF99/papers/TUP031.pdf>
- [3] Z. A. Conway *et al.*, “Achieving high peak fields and low residual resistance in half-wave cavities”, in *Proc. SRF’15*, Whistler, Canada, Sep. 2015, paper WEBA05, pp. 973-975.
<https://jacow.org/SRF2015/papers/WEBA05.pdf>
- [4] D. Luo, K. Saito, and S. Shanab, “Nitrogen contamination causes high field Q-Slope (HFQS) in buffered chemical polished SRF cavities”, arXiv, 2019.
doi:10.48550/ARXIV.1904.00145
- [5] D. Luo, K. Saito, and S. Shanab, “Analysis of high field Q-Slope (HFQS) causes and development of new chemical polishing acid”, in *Proc. NAPAC’2019*, Lansing, MI, USA, pp. 609-702. doi:10.18429/JACoW-NAPAC2019-WEPLM47
- [6] E. Metzgar *et al.*, “Summary of the FRIB electropolishing facility design and commissioning, cavity processing, and cavity test results”, Grand Rapids, MI, USA, Jun. 2023, paper TUPTB016, this conference.
- [7] B. Visentin, “Q-Slope at high gradient: review of experiment and theories”, in *Proc. SRF’03*, 2003.
<https://jacow.org/SRF2003/papers/TU001.pdf>
- [8] K. Saito *et al.*, “Superiority of electropolishing over chemical polishing on high gradients”, in *Proc. of the 1997 Workshop on RF Superconductivity*, Abano Terme (Padova), Italy, 1997, pp. 795-813.
<https://jacow.org/SRF97/papers/SRF97D02.pdf>
- [9] M. Masuzawa, K. Tsuchiya, and A. Terashima, “Study of magnetic shield material and fabrication of magnetic shield for superconducting cavities”, *IEEE Tran. Apply. Sup.*, vol. 24, no. 3, p. 3500104, Jun, 2014.
<https://jacow.org/SRF2013/papers/WEIOD02.pdf>